Neurofuzzy Classification and Rule Generation of Modes of Radiowave Propagation

Swati Choudhury, Sushmita Mitra, *Senior Member, IEEE*, and Sankar K. Pal, *Fellow, IEEE*

***Abstract*—This paper describes, in a neurofuzzy framework, a method for the classification of different modes of radiowave propagation, followed by generation of linguistic rules justifying a decision. Weight decay during neural learning helps in imposing a structure on the network, resulting in the extraction of logical rules. Use of linguistic terms at the input enables better human interpretation of the inferred rules. The effectiveness of the system is demonstrated on radiosonde data of four different seasons in India.**

***Index Terms*—Classification, neurofuzzy approach, rule generation, soft computing.**

I. Introduction

TROPOSPHERIC radiowave propagation is one of the important areas in the field of wireless communications. Radiorefractivity $N(T, P, e, h)$ and the radiorefractivity gradient ΔN are the key parameters to estimate the mode of radiowave propagation, where T, P, e, and h denote the temperature, pressure, vapor pressure, and height, respectively (of the tropospheric region). The radiorefractivity gradient ΔN can be divided into four basic intervals defined as 1) $0 \geq \Delta N \geq -40$ $N-$ units/km, 2) $-40 \geq \Delta N \geq -75$ $N-$ units/km, 3) $-75 \geq \Delta N \geq -157$ $N-$ units/km, and 4) $\Delta N < -157$ $N-$ units/km.

If the estimated ΔN is lying in interval 1, the mode of radiowave propagation is said to be *subrefracted*. Under this mode of propagation, the signal propagating to the receiver experiences a greater loss and sometimes becomes too small to use. The mode of radiowave propagation is said to be *normal* if ΔN lies in interval 2. In the presence of normal refractive conditions, a radiowave travels between a pair of transmitting and receiving antennas with moderate path loss. On the other hand, if ΔN lies in interval 3 or 4, the mode of radiowave propagation is termed as *superrefraction* or *ducting,* respectively. On the occurrence of superrefraction or ducting, the radiowave between a pair of transmitting and receiving antennas propagate with least path loss, which, in turn, improves the reliability and the performance of the system.

Artificial neural networks (ANNs) attempt to replicate the *computational* power (low-level arithmetic processing ability) of biological neural networks and, thereby, hopefully endow machines with some of the (higher level) *cognitive abilities* that biological organisms possess (due in part, perhaps, to their low-level computational prowess). However, an impediment to a more widespread acceptance of ANNs is the absence of a capability to explain to the user, in a form comprehensible to humans, how the network arrives at a particular decision. Recently, there has been widespread activity aimed at redressing this situation by extracting the embedded knowledge in trained ANNs in the form of symbolic rules [1]–[3]. This serves to identify the attributes that, either individually or in combination, are the most significant determinants of the decision or classification.

The connection weights of the trained network are used for extracting refined rules for the problem domain. This helps in minimizing human interaction and associated inherent bias during the phase of knowledge-base formation and also reduces the possibility of generating contradictory rules. The extracted rules help in alleviating the knowledge acquisition *bottleneck,* refining the initial domain knowledge, and providing reasoning and explanation facilities. Fuzzy neural networks [1], used for the same purpose, can also handle uncertainty at various stages. Rules extracted from such networks are more *natural* and can involve linguistic terms in the antecedent and/or consequent clauses.

The objective of this paper is to design a neurofuzzy decision-making system, in a soft computing paradigm, for classification of different modes of radiowave propagation. Rules are extracted to justify a decision. The proposed system is able to exploit the parallelism, self-learning, and fault tolerance characteristics of artificial neural network models while utilizing the uncertainty modeling capability of fuzzy sets. *Soft computing* is a consortium of methodologies that works synergetically and provides, in one form or another, flexible information processing capability for handling real-life ambiguous situations [4]. Its aim is to exploit the tolerance for imprecision, uncertainty, approximate reasoning, and partial truth in order to achieve tractability, robustness, and low-cost solutions. There are ongoing efforts to integrate artificial neural networks with fuzzy set theory, rough set theory, genetic algorithms, and other methodologies in soft computing paradigm [1].

In this investigation, we have used a fuzzy multilayer perception (MLP) [5] to learn the relationship between the input parameters T, P, e, h, T_r, e_r, and h_r and the output class ΔN. Here T_r, e_r, and h_r are the temperature, vapor pressure, and height at the reference level (the height with respect to which the higher level is subrefractive, normal, superrefractive, or ducting). The model helps us in predicting the mode of radiowave propagation from the measure of T, P, e of the tropospheric region at a particular height h. Studies have been made using different network topologies. Links are pruned using weight decay. The learning rate is gradually decreased.

Manuscript received May 16, 2000; revised April 1, 2002.

The authors are with the Machine Intelligence Unit, Indian Statistical Institute, 700035 Calcutta, India (e-mail: swati_v@isical.ac.in; sushmita@isical.ac.in; sankar@isical.ac.in).

Extensive results are presented for various numbers of hidden layers and nodes, using different sizes of training sets for the four major seasons. The trained network is used for subsequent rule generation.

Section II provides a brief review on radio climatology. The fuzzy MLP, used here, is described in Section III for classification and rule generation. The results on radiosonde data over India for the four major seasons are given in Section IV. Section V concludes this paper.

II. Radio Climatology: An Overview

A. Background

Research on radioclimatology solely depends upon the availability of meteorological observations on temperature (T), pressure (P), vapor pressure (e), and various other related parameters. *Radiosonde, instrumented tower,* and *threaded kytoon* [1] are the standard in-situ techniques used to obtain measurements for these parameters. The availability of these data or observations helps the research in the area of radiowave propagation, which is one of the important fields of wireless communications.

To facilitate the research in radioclimatology and radiowave propagation, Kulsrestha and Chatterjee [6]–[9] studied the distribution of surface radiorefractivity N_s and the radiorefractivity at 850 and 700 mb levels based on five years of data collected from 36 surface stations and 12 radiosonde stations situated over India. Srivastava [10] studied the refractivity in the lowest 1 km over India in 1968. During the course of these works, the height resolution was restricted to 1 km in refractivity profiles. In 1974, the height resolution was improved by Majumder by taking refractivity at surface and at 500-m altitude [11].

Prasad [12] has deduced the radio refractive index profiles from radiosonde data collected from 32 stations twice a day (0000 GMT and 1200 GMT) for a period of five years. He has also studied the radioclimatology of some selected regions over India by taking simultaneous observations from kytoon, airborne microwave refractometer, and radar [12]. Measurement of radiosonde data over the eastern coastal belt of India reveals that this region involves significant diurnal, monthly, and seasonal changes, which in turn affect the performance and reliability of different communication systems operating in the higher frequency ranges. Keeping this in mind, Choudhury *et al.* analyzed the radiosonde data over Calcutta to estimate the percentage occurrence of different radiorefractivity gradients during different months and seasons over this region [13], [14].

Apart from this, many scientists have analyzed the radiosonde data and tried to apply the results directly to estimate the useful parameters and factors of radiowave propagation. Rogers [15] designed a useful experiment to study the effects of variability of atmospheric radiorefractivity on propagation estimates. The outcome of his results revealed that, for over-the-horizon overwater electromagnetic propagation calculations at very high and ultrahigh frequencies in the southern California coastal region, the assumption of horizontal homogeneity leads to little more error than the described minimum error. Here minimum error implies the root-mean-square error for estimating the propagation factor. It was observed that estimates based upon range-dependent refractive structures provided substantially less error than estimates based upon homogeneous refractive structures only if they were sampled at intervals of two hours or less. Vasseur [16] measured and analyzed one year's radiosonde data in Belgium. He suggested a new method to estimate the tropospheric scintillation on satellite links. Fruitful research work in the area of radioclimatology and radiowave propagation is being performed also in Japan with rapid progress. In this connection, Manabe and Furuhama have published a very useful review work [17].

[1]Here a kytoon-shaped balloon is not allowed to rise freely but the height is controlled by a nylon cord attached with the balloon. Using this technique, one can make observations up to a height of 2 km.

B. Tropospheric Radiorefractivity and Its Gradient

The tropospheric radiorefractivity at a particular height (h) can be expressed as

$$N = 77.6\frac{P}{T} + 3.75 \times 10^6 \frac{e}{T^2} = \frac{77.6}{T}\left(P + \frac{4810e}{T}\right) \tag{1}$$

where P is the atmospheric pressure in mb, e is the water vapor pressure in mb, and T is the absolute temperature in Kelvin. On the right-hand side of (1), the first term is called the *dry term* and the other the *wet term* [18]. This expression of radiorefractivity is valid up to 100 GHz, with an error less than 0.5%. Likewise, the radiorefractivity of the reference level can be written as

$$N_r = 77.6\frac{P_r}{T_r} + 3.75 \times 10^6 \frac{e_r}{T^2} \tag{2}$$

where the subscript r denotes the reference level.

After the estimation of N and N_r, its gradient ΔN can be calculated as

$$\Delta N = \frac{N - N_r}{h - h_r} \tag{3}$$

where N is the radiorefractivity at higher level, N_r is the radiorefractivity at reference level, h is the height of the higher level, and h_r is the height of the reference level.

III. Fuzzy MLP: Classification and Rule Generation

The fuzzy MLP model [5] incorporates fuzziness at the input and output levels of the MLP and is capable of handling exact (numerical) and/or inexact (linguistic) forms of input data. Any input feature value is described in terms of some combination of membership values in the linguistic property sets *low* (L), *medium* (M), and *high* (H). Class membership values (μ) of patterns are represented at the output layer of the fuzzy MLP. During training, the weights are updated by backpropagating errors with respect to these membership values such that the contribution of uncertain vectors is automatically reduced. A schematic diagram depicting the whole procedure is provided in Fig. 1. The various phases of the algorithm are described below. Rules are generated from the trained network.

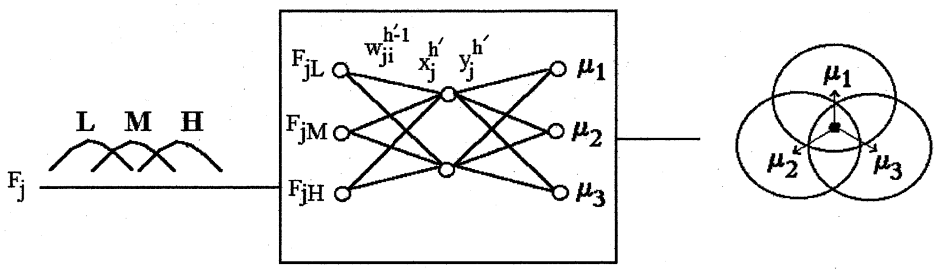

Fig. 1. Block diagram of fuzzy MLP.

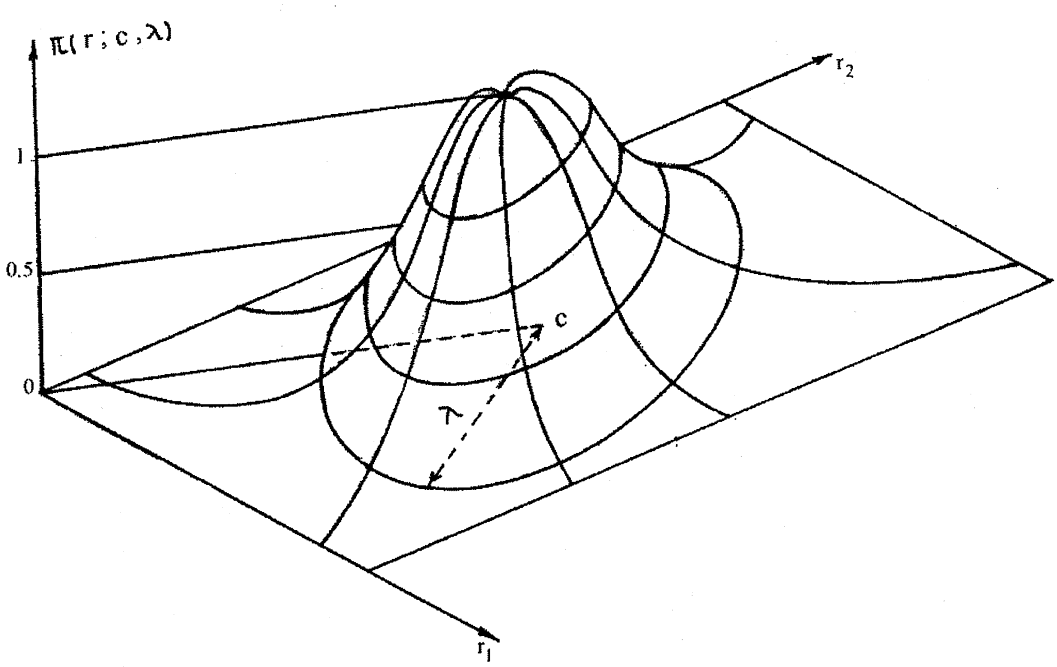

Fig. 2. The π-set.

A three-layered feed-forward MLP is used. The output of a neuron in any layer (h) other than the input layer $(h' = 0)$ is given as

$$y_j^{h'} = \frac{1}{1 + \exp\left(-\sum_i y_i^{h'-1} w_{ji}^{h'-1}\right)} \tag{4}$$

where $y_i^{h'-1}$ is the state of the ith neuron in the preceding $(h'-1)$th layer and $w_{ji}^{h'-1}$ is the weight of the connection from the ith neuron in layer $h'-1$ to the jth neuron in layer h'. For nodes in the input layer, y_j^0 corresponds to the jth component of the input vector. Note that $x_j^{h'} = \sum_i y_i^{h'-1} w_{ji}^{h'-1}$.

A. Input Vector

An n-dimensional pattern $\mathbf{F}_i = [F_{i1}, F_{i2}, \ldots, F_{in}]$ is represented as a $3n$-dimensional vector

$$\mathbf{F}_i = \left[\mu_{low(F_{i1})}(\mathbf{F}_i), \ldots \mu_{\text{high}(F_{in})}(\mathbf{F}_i)\right] = \left[y_1^0, y_2^0, \ldots, y_{3n}^0\right] \tag{5}$$

where μ indicates the membership function of the corresponding linguistic π-sets *low, medium,* and *high* along each feature axis and $y_1^0, \ldots, y_{3n}^0$ refer to the activations of the $3n$ neurons in the input layer.

When the input feature is numerical, we use the π-fuzzy sets (in the one dimensional form), with range [0,1] represented as

$$\pi(F_j; c, \lambda) = \begin{cases} 2\left(1 - \frac{\|F_j - c\|}{\lambda}\right)^2, & \text{for } \frac{\lambda}{2} \le \|F_j - c\| \le \lambda \\ 1 - 2\left(\frac{\|F_j - c\|}{\lambda}\right)^2, & \text{for } 0 \le \|F_j - c\| \le \frac{\lambda}{2} \\ 0, & \text{otherwise} \end{cases} \tag{6}$$

where $\lambda(> 0)$ is the radius of the π-function with c as the central point. This is shown in Fig. 2. Note that features in linguistic and set forms can also be handled in this framework [5].

Hence, in trying to express an input $\boldsymbol{F}_i$ with linguistic properties, one effectively divides the dynamic range of each feature into three overlapping partitions, as in Fig. 3. The centers and radii of the π functions along each feature axis are determined automatically from the distribution of the training patterns.

B. Output Representation

Let the n-dimensional vectors $\mathbf{o}_k = [o_{k1} \ldots o_{kn}]$ and $\mathbf{v}_k = [v_{k1}, \ldots, v_{kn}]$ denote the mean and standard deviation, respectively, of the numerical training data for the kth class c_k. The

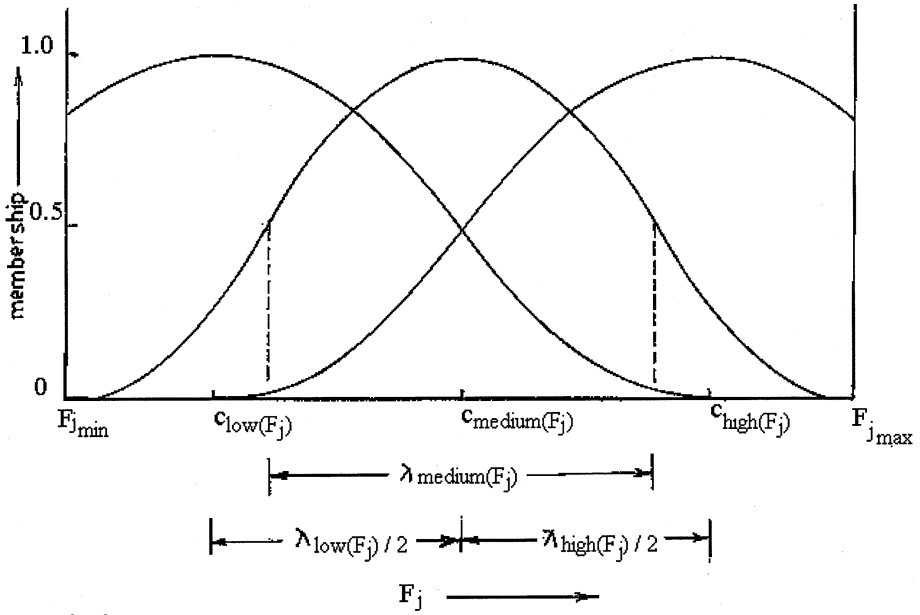

Fig. 3. Overlapping structure of π functions.

weighted distance of the training pattern $\mathbf{F}_i$ from the kth class c_k is defined as

$$z_{ik} = \sqrt{\sum_{j=1}^{n} \left[\frac{F_{ij} - o_{kj}}{V_{kj}} \right]^2} \tag{7}$$

where F_{ij} is the value of the jth component of the ith pattern point.

The membership of the ith pattern in class k, lying in the range [0,1], is defined as [19]

$$\mu_k(\mathbf{F}_i) = \frac{1}{1 + \left(\frac{z_{ik}}{f_d} \right)^{f_e}} \tag{8}$$

where positive constants f_d and f_e are the denominational and exponential fuzzy generators controlling the amount of fuzziness in the class membership set and $k \in \{1, \ldots, l\}$ for an l-class problem with l output nodes.

C. Rule Generation

In general, the primary input to a connectionist rule generation algorithm is a representation of the trained ANN, in terms of its nodes and links, and sometimes the data set. One interprets one or more hidden and output units into rules, which may later be combined and simplified to arrive at a more comprehensible rule set. These rules can also provide new insights into the application domain. The use of ANN helps in 1) incorporating parallelism and 2) tackling optimization problems in the data domain. Fuzzy neural networks [1] can be used for the same purpose and can also handle uncertainty at various stages.

The fuzzy MLP is trained using backpropagation and the connection weights pruned with weight decay. The trained network is next analyzed for rule generation. The strong paths from the output nodes (classes) to the input (features), i.e., those paths having large magnitude, are extracted. We consider both positive and negative link weights in the process. The antecedents of the rules are in terms of the linguistic values at the input to which the path can be traced.

Algorithms for rule generation from neural networks mainly fall into two categories—pedagogical and decompositional [3]. Our algorithm for rule extraction [20], [21] can be categorized as decompositional. It is described below.

1) Compute the following quantities:
   $PMean$ = mean of all positive weights, $PThres_1$ = mean of all positive weights less than$PMean$,
   $PThres_2$ = mean of all weights greater than $PMean$.
   Similarly calculate $NThres_1$ and $NThres_2$ for negative weights.
2) For each hidden and output unit:
   (a) For all weights greater than $PThres_2$ search for positive rules only, and for all weights less than $NThres_2$ search for negated rules only by *Subset* method.
   (b) Search for combinations of positive weights above $PMean$ and negative weights greater than $NThres_2$ that exceed the bias. Similarly search for negative weights less than $NMean$ and positive weights below $PThres_2$ to generate rules.

The *Subset* method [22] conducts a breadth first search for all the hidden and output nodes over the input links. The algorithm starts by determining whether any sets containing a single link are sufficient to guarantee that the bias is exceeded. If yes, then these sets are rewritten as rules in disjunctive normal form. The search proceeds by increasing the size of the subsets until all possible subsets have been explored. Finally, the algorithm removes subsumed and overly general rules.

Let us now explain our algorithm with a simple example. We consider weights having value greater than $PThres_2$ as strong connections [plotted as thick lines for a sample network, as shown in Fig. 4(a)] and weights having value between $PMean$ and $PThres_2$ as moderate links (plotted as normal lines in the figure). We obtained $PThres_1 = 81.95$,

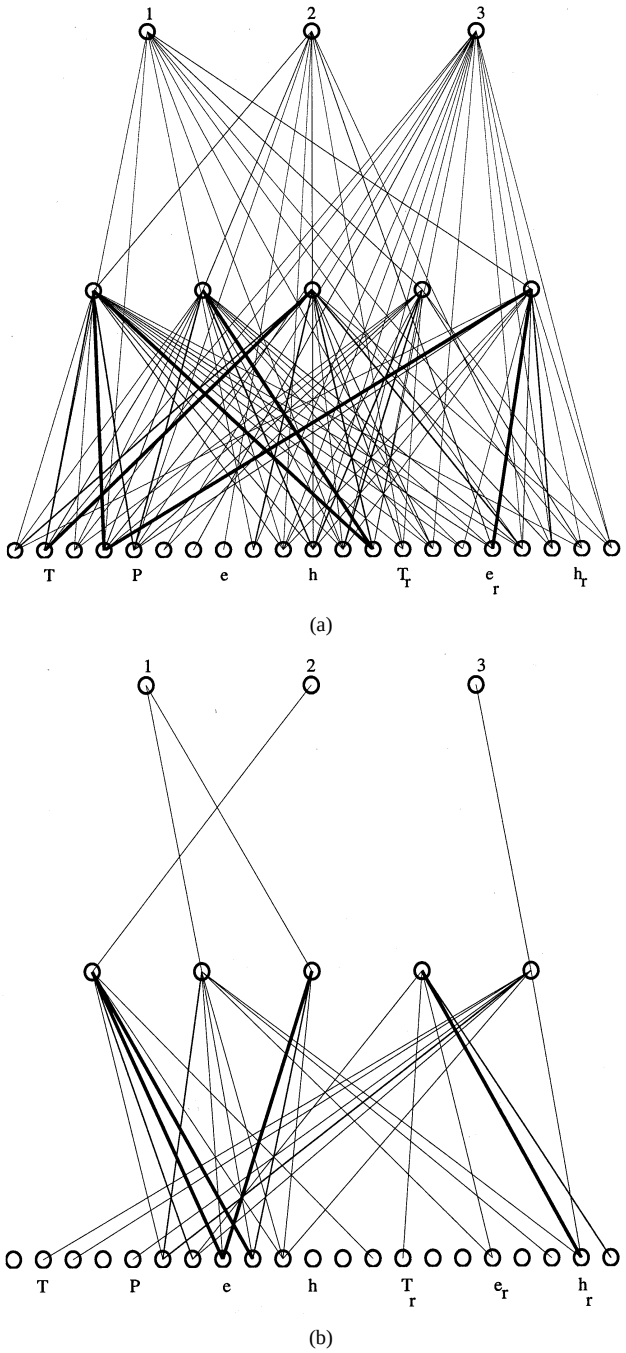

Fig. 4. (a) Positive and (b) negative connectivity of fuzzy MLP for *Post-Monsoon* data.

$PMean = 161.18$, and $PThres_2 = 220.23$. Similarly calculate $NThres_1$, $NMean$, and $NThres_2$ for negative weights. The corresponding network (representing only the negative links) is provided in Fig. 4(b), with $NThres_1 = -84.30$, $NTMean = -162.64$, and $NThres_2 = -279.46$.

IV. Results

The radiosonde data consist of a set of 1440 patterns obtained from the database of the Indian Meteorological Department, Calcutta. There are four seasons: *Post-Monsoon, Winter, Pre-Monsoon,* and *Monsoon,* each contributing 360 pattern points. The seven input features correspond to temperature (T), pressure (P), vapor pressure (e), height (h), temperature at reference level (T_r), vapor pressure at reference level (e_r), and height of the reference level (h_r). The four intervals for ΔN are mapped to three output classes, clubbing intervals 3, 4 to class 3 only. These classes refer to subrefraction, normal refraction, and superrefraction and ducting, and are denoted as 1, 2, 3, respectively, in the results. The input features are split into 21 components in the linguistic space of (5). Cross-validation of results is made with atmospheric science experts.

Various three-layered networks were used with different numbers of hidden nodes and training sets. The training set size $x\%$ refers to random, class-wise selection of $x\%$ training data from the entire dataset. The remaining $100{-}x\%$ data constitute the test set in each case. Different random initializations were made, and consistent results were obtained for classification and rule generation.

Tables I–IV provide the classification results for the *Post-Monsoon, Winter, Pre-Monsoon,* and *Monsoon* data, respectively, for $x = 50, 60, 70$ and hidden nodes 2, 3, 4, 5, 6. The mean square error refers to the squared error between the desired and computed outputs at the output layer of the network, averaged over the test set under consideration. Sets of refined rules extracted from the network, considering only the strong and moderate links, are also presented.

Fig. 4 depicts the positive and negative connectivity of a pruned fuzzy MLP with five hidden nodes and 60% and 70% training set, respectively, for *Post-Monsoon* data. Extracted rules are as follows.

- For class 1 (subrefractive):
  Positive: If T is *medium,* P is *low* or *medium,* T_r is *low,* h is *medium* or *high,* e_r is *medium,* h_r is *low;*
  Negative: If P is not *high,* e is not *medium* or *high.*
- For class 2 (normal-refractive):
  Positive: If T is *low* or *medium,* P is *low* or *medium,* T_r is *low,* h is *medium,* e is *high,* e_r is *high;*
  Negative: If e is not *medium* or *high.*
- For class 3 (superrefractive):
  Positive: If P is *low,* e_r is *medium,* h_r is *low.*

The validity of the extracted rules can be cross-examined on the basis of experimental result obtained from the analysis of radiosonde data as well as on the basis of mathematical verification of the well-established relations of refractivity and its gradient [(1)–(3)]. The expression of refractivity implies that the radiorefractivity is directly proportional to pressure P and vapor pressure e, and inversely proportional to temperature T and its square term T^2. It also shows that the vapor pressure e contributes very largely to radiorefractivity, as it is multiplied by a very high numerical value. Moreover, the expression for radiorefractivity gradient [(3)] depicts that the condition of subrefraction will be fulfilled when the radiorefractivity gradient ΔN is less negative or positive. To satisfy this condition, mathematically the radiorefractivity at reference level N_r must be slightly greater or smaller than that of radiorefractivity at higher level N. Similarly, for normal-refraction, N_r must be moderately greater than N. On the other hand, for superrefraction and ducting, N_r

TABLE I
RECOGNITION SCORES WITH FUZZY MLP FOR *POST-MONSOON* DATA

Training set size	No. of hidden nodes	training set class 1	class 2	class 3	net	testing set class 1	class 2	class 3	net	mean square error
50%	2	66.67	94.83	61.54	85.21	40.00	84.72	49.02	71.94	0.0829
	3	70.37	96.55	65.38	87.57	43.64	86.90	45.10	73.43	0.0732
	4	88.89	99.14	76.92	94.08	52.73	86.90	47.06	75.22	0.0492
	5	96.30	100.00	76.92	95.86	54.55	87.77	49.02	76.42	0.0368
	6	100.00	100.00	73.08	95.86	58.18	87.34	50.98	77.01	0.0314
60%	2	51.52	96.40	61.29	83.74	40.00	89.96	54.90	76.42	0.0873
	3	54.55	97.12	80.65	87.68	40.00	88.21	62.75	76.42	0.0746
	4	75.76	99.28	67.74	90.64	54.55	91.27	54.90	79.70	0.0589
	5	90.91	100.00	74.19	94.58	63.64	93.01	56.86	82.69	0.0385
	6	96.97	100.00	70.97	95.07	67.27	89.52	54.90	80.60	0.0356
70%	2	83.49	78.43	69.23	79.20	79.22	68.28	58.93	71.55	0.1042
	3	83.49	63.73	76.92	74.40	76.62	53.79	62.50	65.07	0.1280
	4	91.74	90.20	82.05	89.60	83.12	80.00	64.29	78.87	0.0688
	5	76.32	98.16	83.33	92.41	61.82	87.77	70.59	80.90	0.0591
	6	89.47	99.39	83.33	95.36	69.09	90.39	66.67	83.28	0.0435

TABLE II
RECOGNITION SCORES WITH FUZZY MLP FOR *WINTER* DATA

Training set size	No. of hidden nodes	training set class 1	class 2	class 3	net	testing set class 1	class 2	class 3	net	mean square error
50%	2	83.10	83.12	55.56	81.53	67.38	69.33	50.00	67.31	0.1017
	3	92.96	92.21	77.78	91.72	71.63	71.33	55.56	70.55	0.0617
	4	95.77	92.21	77.78	92.99	78.72	62.00	65.56	69.26	0.0628
	5	92.96	94.81	77.78	92.99	75.89	68.67	61.11	71.52	0.0620
	6	98.59	97.40	88.89	97.45	77.30	74.67	66.67	75.40	0.0328
60%	2	87.06	78.26	60.00	81.28	80.58	64.45	55.56	72.17	0.0910
	3	94.12	92.39	80.00	92.51	77.70	69.08	61.11	72.49	0.0572
	4	95.29	96.74	70.00	94.65	84.17	77.63	61.11	79.61	0.0544
	5	98.82	95.65	70.00	95.72	79.86	73.03	38.89	74.11	0.0490
	6	97.65	97.83	88.00	96.79	84.17	80.92	66.67	81.55	0.0379
70%	2	76.77	67.29	25.00	69.27	77.70	64.05	29.41	68.28	0.1168
	3	88.89	85.98	50.00	85.32	80.58	75.82	52.94	76.70	0.0880
	4	90.91	87.85	75.00	88.53	80.58	79.74	70.59	79.61	0.0696
	5	95.96	94.39	83.33	94.50	82.73	79.05	58.82	79.61	0.0474
	6	97.98	97.20	83.33	96.79	88.49	81.05	70.59	83.82	0.0336

must be significantly greater than N, so that ΔN may become more and more negative.

The extracted positive rule for *Post-Monsoon* season (class 1) shows that the subrefractive condition prevails when temperature T at higher level is medium, pressure P is low or medium, the temperature at reference level T_r is low, the vapor pressure at reference level e_r is medium, the height of the higher level h is medium or high, and the height of the reference level h_r is low. The analyzed radiosonde data for the *Post-Monsoon* season were thoroughly scrutinized, and it was observed that the occurrence of this type of combination of atmospheric parameters leads to formation of subrefractive gradients for the majority of cases. On the other hand, theoretically, this type of combination suggests that the radiorefractivity at the higher level N will be medium, whereas the radiorefractivity at the reference level N_r will be moderately high (because e_r is medium and T_r is low). Therefore, the term $N - N_r$ in (3) will be a moderately negative term and the term $h - h_r$ will be medium or high (because h is

TABLE III
RECOGNITION SCORES WITH FUZZY MLP FOR *PRE-MONSOON* DATA

Training set size	No. of hidden nodes	training set class 1	2	3	net	testing set class 1	2	3	net	mean square error
	2	84.62	93.15	67.86	85.47	72.23	71.72	53.57	69.30	0.0789
	3	89.74	94.52	64.29	87.71	75.32	74.48	41.07	69.58	0.0666
50%	4	97.44	98.63	67.86	93.30	77.92	76.55	41.07	71.55	0.0500
	5	97.44	100.00	75.00	94.97	80.52	79.31	48.21	74.93	0.0400
	6	96.15	98.63	78.57	94.41	80.52	73.10	51.79	72.96	0.0408
	2	82.98	82.95	63.64	80.00	75.32	73.10	50.00	70.42	0.0933
	3	88.30	90.91	69.70	86.51	78.54	75.17	57.14	74.37	0.0740
60%	4	93.62	89.77	75.76	89.30	83.77	75.86	55.36	76.06	0.0639
	5	95.74	93.18	63.64	89.77	85.06	80.00	51.79	77.75	0.0593
	6	97.87	100.00	78.79	95.81	84.42	82.07	53.57	78.59	0.0374
	2	82.57	73.53	69.23	76.80	80.52	68.28	60.71	72.39	0.1050
	3	88.99	87.25	74.36	86.00	83.12	79.31	62.50	78.31	0.0852
70%	4	91.74	90.20	82.05	89.60	83.12	80.00	64.29	78.87	0.0688
	5	98.17	95.10	76.92	93.60	88.96	80.00	58.93	80.56	0.0475
	6	96.33	93.14	87.18	93.60	87.01	79.31	66.07	80.56	0.0518

TABLE IV
RECOGNITION SCORES WITH FUZZY MLP FOR *MONSOON* DATA

Training set size	No. of hidden nodes	training set class 1	2	3	net	testing set class 1	2	3	net	mean square error
	2	75.00	96.70	72.73	92.11	48.00	84.90	52.38	77.43	0.0648
	3	91.67	98.90	72.73	95.61	60.00	87.78	52.38	81.42	0.0521
50%	4	83.33	98.90	72.73	94.74	64.00	86.67	57.14	81.42	0.0498
	5	75.00	96.70	63.64	91.32	52.00	86.67	38.10	78.32	0.0604
	6	91.67	100.00	63.44	95.61	64.00	88.89	38.10	81.42	0.0449
	2	53.33	92.66	61.54	85.40	32.00	86.74	50.00	77.43	0.0762
	3	73.33	96.33	76.92	91.97	48.00	93.37	76.92	84.51	0.0575
60%	4	80.00	97.25	61.54	91.97	56.00	95.03	40.00	85.84	0.0563
	5	66.67	90.83	69.23	86.13	48.00	88.40	50.00	80.53	0.0624
	6	80.00	93.8	69.23	89.78	56.00	90.06	50.00	82.74	0.0634
	2	47.06	96.09	66.67	88.12	40.00	93.92	60.00	84.96	0.0685
	3	82.35	99.22	86.67	96.25	60.00	95.58	55.00	88.05	0.0419
70%	4	82.35	98.44	86.67	95.62	60.00	93.92	65.00	87.61	0.0400
	5	64.71	96.09	80.00	91.25	52.00	91.71	50.00	83.63	0.0535
	6	70.59	96.88	73.33	91.88	52.00	93.37	50.00	84.96	0.0526

medium or high and h_r is low). On dividing, this contributes to a less negative value for ΔN, usually lying in the subrefractive range.

This positive rule is also well supported by the negative rule, which suggests that in *Post-Monsoon* season the subrefractive condition will not occur when the vapor pressure e at the higher level is not medium or high, i.e., e is low. Now if e is low, then N will be low and $N - N_r$ will be more negative, which practically indicates the occurrence of superrefraction or ducting. In support of this, an investigation on analyzed radiosonde data for this season also shows that if the vapor pressure gradient is negative, i.e., the vapor pressure decreases with height, then the probability of formation of superrefractive gradient is very high. Likewise, the rest of the generated rules are verified for this season as well as for the other three. We do not go into their details here because of space constraints. It is observed that there exists a very good agreement between the generated rules and the recorded radiosonde observations.

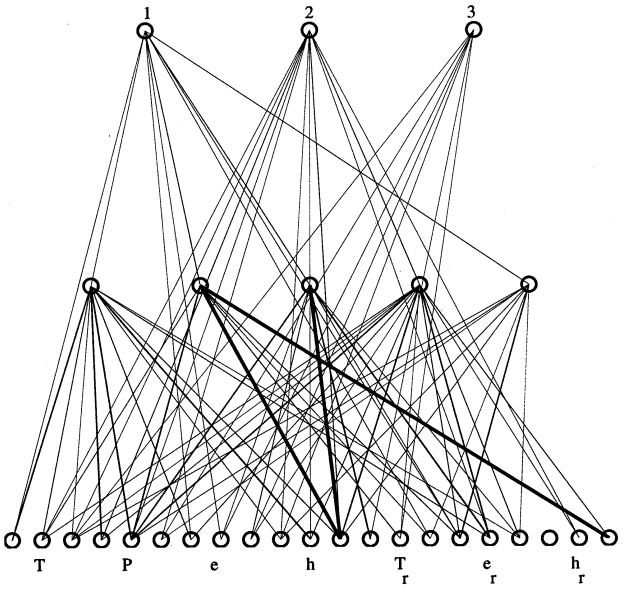

(a)

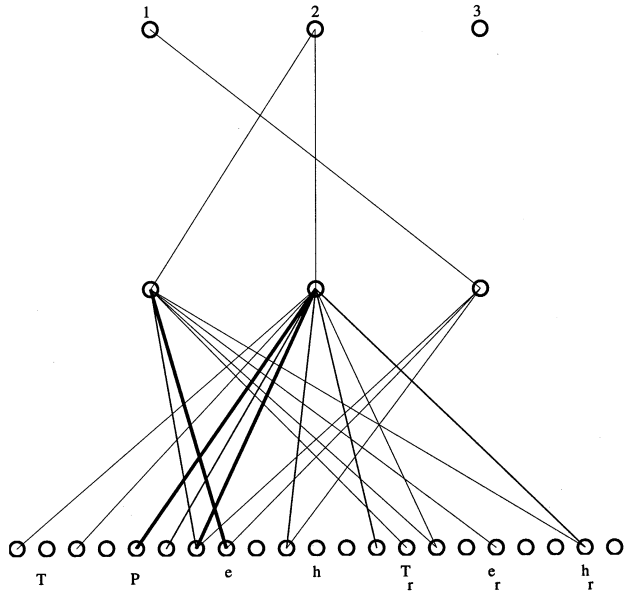

(b)

Fig. 5. (a) Positive and (b) negative connectivity of fuzzy MLP for *Winter* data.

Fig. 5 depicts the positive and negative connectivity of a pruned fuzzy MLP with five and three hidden nodes and 50% and 60% training set, respectively, for *Winter* data. Sample extracted rules are as follows.

- For class 1 (subrefractive):
  Positive: If T is *low*, P is *low* or *medium*, h_r is *high*, h is *medium* or *high*, e_r is *low* or *medium*.
- For class 2 (normal-refractive):
  Positive: If P is *medium*, h is *high*, e_r is *medium;*
  Negative: If P is not *medium* or *high*, h is not *low*, T_r is not *low*, e is not *low*, h_r is not *medium*.
- For class 3 (superrefractive):
  Positive: If T is *high*, P is *high*, e is *medium* or *high*, h is *low*, T_r is *low* or *medium*.

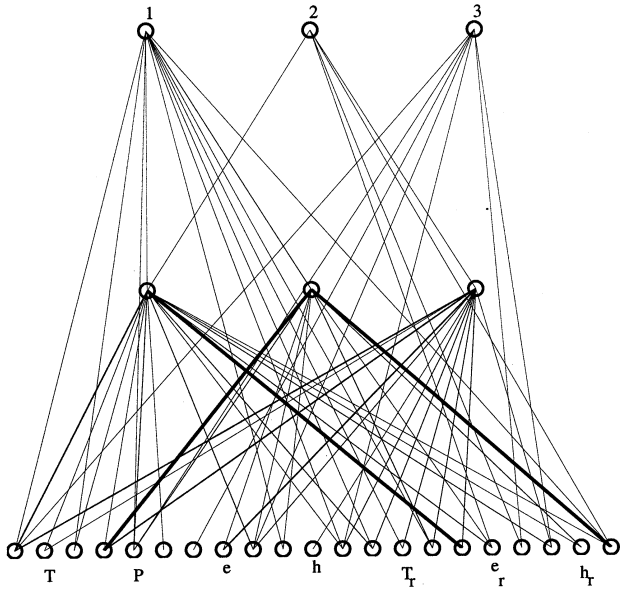

(a)

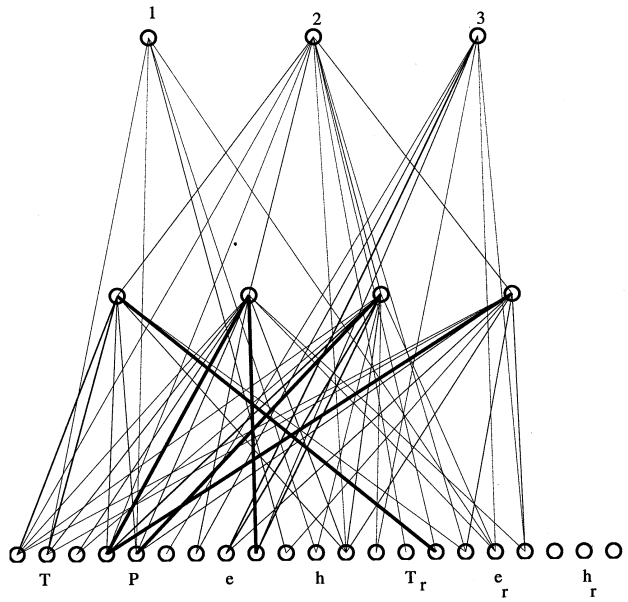

(b)

Fig. 6. Positive connectivity of fuzzy MLP for (a) *Pre-Monsoon* and (b) *Monsoon* data.

Fig. 6(a) depicts the connectivity of a pruned fuzzy MLP with three hidden nodes and 70% training set for *Pre-Monsoon* data. Positive rules extracted from this trained network are as follows.

- For class 1 (subrefractive):
  If T is *low*, e_r is *low*, P is *low*, h_r is *high*.
- For class 2 (normal-refractive):
  If T is *low*, e_r is *low*, P is *low*, e is *medium*.
- For class 3 (superrefractive):
  If T is *low*, P is *medium*, e is *low* or *medium*, h is *high*, e_r is *high*, h_r is *low*.

Fig. 6(b) depicts the connectivity of a pruned fuzzy MLP with four hidden nodes and 70% training set for *Monsoon* data. Sample positive rules extracted from this trained network are as follows.

- For class 1 (subrefractive):
  If T is *medium*, P is *medium*, T_r is *low*, h is *low* or *medium*, e_r is *medium*.
- For class 2 (normal-refractive):
  If T is *low* or *medium*, T_r is *high*, P is *low* or *medium*, e is *medium* or *high*.

V. Conclusion

We have described a method of linguistic rule generation for categorizing the modes of radiowave propagation in a neurofuzzy framework. The fuzzy MLP used here learns the relationship between the input parameters T, P, e, h and the output class ΔN. Studies have been made using different network topologies. The extracted rules are used to justify inferred decisions. These have been verified with the radiosonde observations recorded over Calcutta during four different seasons. It has been found that there exists a good agreement between the generated rules and recorded observations.

The use of the fuzzy MLP enables one to estimate the refractive condition of the higher level (N) in the experiments, even in the absence of P_r of (2). The practical utility of this aspect is that the robustness inherent in neural net architecture is able to handle missing data, possibly caused by malfunctioning of radiosonde equipments.

It is concluded that said neurofuzzy approach, involving rule generation, is useful in assessing the radiorefractive condition of the tropospheric boundary layer. This enables the speculation of radiowave signal situation at the receiver's site. The extracted knowledge can be used to set up ground-based radio communication link over a region. The resultant model will also be advantageous to researchers working in remote sensing, atmospheric science, and various other related fields.

References

[1] S. K. Pal and S. Mitra, *Neuro-Fuzzy Pattern Recognition: Methods in Soft Computing*. New York: Wiley, 1999.

[2] S. Mitra and Y. Hayashi, "Neuro-fuzzy rule generation: survey in soft computing framework," *IEEE Trans. Neural Networks*, vol. 11, pp. 748–768, 2000.

[3] R. Andrews, J. Diederich, and A. B. Tickle, "A survey and critique of techniques for extracting rules from trained artificial neural networks," *Knowledge-Based Syst.*, vol. 8, pp. 373–389, 1995.

[4] L. A. Zadeh, "Fuzzy logic, neural networks, and soft computing," *Commun. ACM*, vol. 37, pp. 77–84, 1994.

[5] S. K. Pal and S. Mitra, "Multi-layer perception, fuzzy sets and classification," *IEEE Trans. Neural Networks*, vol. 3, pp. 683–697, 1992.

[6] S. M. Kulsrestha and K. Chatterjee, "Radioclimatology of India: 1. Radio refractive index near the ground surface," *Ind. J. Met. Geophys.*, vol. 17, no. 2, p. 367, 1966.

[7] ——, "Radioclimatology of India: 2. Radio refractive index near ground surface," *Ind. J. Met. Geophys.*, vol. 17, no. 2, p. 545, 1966.

[8] ——, "Radioclimatology of India: 3. Radio refractive index at 700 mb level," *Ind. J. Met. Geophys.*, vol. 18, no. 2, p. 185, 1967.

[9] ——, "Radioclimatology of India: 4. Vertical structure of radio refractive index distribution in the lower troposphere," *Ind. J. Met. Geophys.*, vol. 18, no. 3, p. 335, 1967.

[10] H. N. Srivastava, "Refractivity in the lowest 1 km. over India," *Ind. J. Pure Appl. Phys.*, vol. 25, 1968.

[11] S. C. Majumder, "Some observations on distance dependence in tropospheric propagation beyond the radio horizon," *Radio Electron. Eng.*, vol. 44, p. 63, 1974.

[12] M. Prasad, "Some aspects of VHF and microwave propagation over selected regions of India and their application to communication," National Physical Lab., New Delhi, India, CENTROP Rep. 50, 1989.

[13] S. Choudhury, A. Pal, and D. Dutta Majumder, "Tropospheric VHF propagation studies over Indian east coast," *Ind. J. Phys.*, vol. 72B, no. 6, pp. 571–608, 1998.

[14] S. Choudhury and D. Dutta Majumder, "Radioenvironment over Indian east coast: a combined study from sonar observations and radiosonde measurements," *Ind. J. Phys.*, vol. 73B, no. 3, pp. 423–461, 1999.

[15] L. T. Rogers, "Effects of the variability of atmospheric refractivity on propagation estimates," *IEEE Trans. Antennas Propagat.*, vol. 44, pp. 460–465, 1996.

[16] H. Vasseur, "Prediction of tropospheric scintillation on satellite links from radiosonde data," *IEEE Trans. Antennas Propagat.*, vol. 47, pp. 293–301, 1999.

[17] T. Manabe and Y. Furuhama, "Recent propagation studies in Japan," *IEEE Trans. Antennas Propagat.*, vol. 36, pp. 7–13, 1994.

[18] B. R. Bean and E. J. Dutton, "Concerning radiosonde, lag constants and refractive index profiles," *J. Geophys. Res.*, vol. 66, no. 11, pp. 3711–3722, 1961.

[19] S. K. Pal and D. Dutta Majumder, *Fuzzy Mathematical Approach to Pattern Recognition*. New York: Wiley/Halsted, 1986.

[20] P. Mitra, S. Mitra, and S. K. Pal, "Staging of cervical cancer with soft computing," *IEEE Trans. Biomed. Eng.*, vol. 47, pp. 934–940, 2000.

[21] S. K. Pal, S. Mitra, and P. Mitra, "Rough fuzzy MLP: modular evolution, rule generation and evaluation," *IEEE Trans. Knowledge Data Eng.*, vol. 15, pp. 14–25, 2003.

[22] L. M. Fu, "Knowledge-based connectionism for revising domain theories," *IEEE Trans. Syst., Man, Cybern.*, vol. 23, pp. 173–182, 1993.

Swati Choudhury received the M.Sc. degree in physics (electronics) from Rohilkhand University, Bareilly, India, the M.Phil. degree in physical science from S. N. Bose Institute of Physical Sciences, Calcutta, India, and the Ph.D. degree in radio physics and electronics from the University of Calcutta, India, in 2000.

She joined the Electronics and Communication Sciences Unit of Indian Statistical Institute (ISI), Calcutta, and is currently with the Machine Intelligence Unit. Her areas of research interest include neural networks, radio communication, atmospheric remote sensing, radio climatology, and air-pollution meteorology.

Sushmita Mitra (M'99–SM'01) received the B.Sc. (Hons.) degree in physics and the B.Tech. and M.Tech. degrees in computer science from the University of Calcutta, Calcutta, India, in 1984, 1987, and 1989, respectively, and the Ph.D. degree in computer science from Indian Statistical Institute (ISI), Calcutta, in 1995.

She is an Associate Professor at ISI. During 1992–1999, she was with the European Laboratory for Intelligent Techniques Engineering, Aachen, Germany, as a German Academic Exchange Service (DAAD) Fellow. She is the author of *Neuro-Fuzzy Pattern Recognition: Methods in Soft Computing Paradigm* (New York: Wiley, 1999). She was a Visiting Professor at Meiji University, Japan, in 1999 and at Aalborg University, Esbjerg, Denmark, in 2002. Her research interests include pattern recognition, fuzzy sets, artificial intelligence, data mining, neural networks, soft computing, and bioinformatics. She has published approximately 50 research papers in international journals and conference proceedings.

Dr. Mitra received the National Talent Search Scholarship (1978–1983) from the National Council for Educational Research and Training, India, the IEEE TNN Outstanding Paper Award in 1994, and a CIMPA-INRIA-UNESCO Fellowship in 1996.

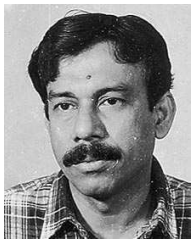

Sankar K. Pal (M'81–SM'84–F'93) received the M.Tech. and Ph.D. degrees in radio physics and electronics from the University of Calcutta, India, in 1974 and 1979, respectively, and the Ph.D. degree in electrical engineering and the Diploma of Imperial College, University of London, U.K., in 1982.

He is a Distinguished Scientist and Founding Head of the Machine Intelligence Unit, Indian Statistical Institute, Calcutta. He was with the University of California, Berkeley, and the University of Maryland, College Park, during 1986–1987 as a Fulbright Postdoctoral Visiting Fellow; with the NASA Johnson Space Center, Houston, TX, during 1990–1992 and 1994 as a Guest Investigator under the NRC-NASA Senior Research Associateship program; and with the Hong Kong Polytechnic University, Hong Kong, in 1999 and 2000 as a Visiting Professor. He was a Distinguished Visitor of the IEEE Computer Society (USA) for the Asia-Pacific Region during 1997–1999, delivering lectures in Australia, Singapore, and China. His research interests include pattern recognition, image processing, soft computing, neural nets, genetic algorithms, and fuzzy systems. He is a coauthor of six books, including *Fuzzy Mathematical Approach to Pattern Recognition* (New York: Wiley/Halsted, 1986) and *Neuro-Fuzzy Pattern Recognition: Methods in Soft Computing* (New York: Wiley, 1999), and has about 300 research publications.

Prof. Pal is a Fellow of the Third World Academy of Sciences, Italy, and all four National Academies for Science/Engineering in India. He received the 1990 S. S. Bhatnagar Prize, the 1993 Jawaharlal Nehru Fellowship, the 1993 Vikram Sarabhai Research Award, the 1993 NASA Tech Brief Award, the 1994 IEEE TRANSACTIONS ON NEURAL NETWORKS Outstanding Paper Award, the 1995 NASA Patent Application Award, the 1997 IETE-Ram Lal Wadhwa Gold Medal, the 1998 Om Bhasin Foundation Award, the 1999 G. D. Birla Award for Scientific Research, the 2000 Khwarizmi International Award (first winner) from the Islamic Republic of Iran, the 2001 Syed Husain Zaheer Medal from Indian National Science Academy, and the 2001 FICCI Award for Engineering and Technology from the Federation of Indian Chamber of Commerce and Industries, India. He is an Associate Editor of the IEEE TRANSACTIONS ON NEURAL NETWORKS and IEEE TRANSACTIONS ON PATTERN ANALYSIS AND MACHINE INTELLIGENCE, *Pattern Recognition Letters*, *International Journal of Pattern Recognition and Artificial Intelligence*, *Neurocomputing*, *Applied Intelligence*, *Information Sciences*, *Fuzzy Sets and Systems*, and *Fundamenta Informaticae*. He is a Member of the Executive Advisory Editorial Board, IEEE TRANSACTIONS ON FUZZY SYSTEMS, *International Journal on Image and Graphics*, and *International Journal of Approximate Reasoning*. He has been a Guest Editor of many journals, including IEEE COMPUTER.